Magnetic mineral diagenesis in the post-glacial muddy sediments from the southeastern South Yellow Sea: Response to marine environmental changes

LIU Jian[1,2], ZHU Rixiang[2], LI Shaoquan[1] & Jeong-Hae Chang[3]

1. Qingdao Institute of Marine Geology, Qingdao 266071, China;
2. Institute of Geology and Geophysics, Chinese Academy of Sciences, Beijing 100029, China;
3. Korean Institute of Geology, Mining & Material, Taejon, Korea;
Correspondence should be addressed to Liu Jian (email: liujian0550@vip.sina.com)

Received November 25, 2002

Abstract Core YSDP103 was retrieved in the muddy deposit under the cold eddy of the southeastern South Yellow Sea, and the uppermost 29.79 m core represents the muddy sediments formed in the shelf since about 13 ka BP. The lower part from 29.79 to 13.35 m, called Unit A2, was deposited during the period from the post-glacial transgression to the middle Holocene (at about 6 ^{14}C ka BP) when the rising sea level reached its maximum, while the upper part above 13.35 m (called Unit A1) was deposited in a cold eddy associated with the formation of the Yellow Sea Warm Current just after the peak of post-glacial sea level rise. Rock-magnetic properties of the uppermost 29.79 m core were investigated in detail. The experimental results indicate that the magnetic mineralogy of the core is dominated by magnetite, maghemite and hematite and that, except for the uppermost 2.35 m, the magnetic minerals were subject to reductive diagenesis leading to significant decline of magnetic mineral content and the proportion of low-coercivity component. More importantly, ferrimagnetic iron sulphide (greigite) is found in Unit A2 but absent in Unit A1, suggesting the control of marine environmental conditions on the magnetic mineral diagenesis. Magnetic parameters show abrupt changes across the boundary between Units A1 and A2, which reflects a co-effect of environmental conditions and primary magnetic components of the sediments on the diagenesis. Alternating zones of high and low magnetic parameters are observed in Unit A2, which is presumably due to periodic changes of the concentration and/or grain size of magnetic minerals carried into the study area.

Keywords: environmental magnetism, magnetic minerals, diagenesis, ferrimagnetic iron sulphide, South Yellow Sea.

DOI: 10.1360/02yd0302

During the last two decades, environmental magnetic studies have had one of the emphases put on the early diagenesis of sediments which results in the dissolution and phase alternation of magnetic minerals incorporated in the sediments[1—3]. This is because the diagenetic changes of magnetic minerals can not only affect the reliability of paleomagnetic records[4] but also bear environmental significance[5, 6]. International researches in this field have been mainly concentrated on deep-water marine sediments such as those deposited in the continental margins[7], hemipelagic[8] and pelagic areas[9], and on lake sediments[5,10]. Chinese

scholars have seldom set feet in the studies of diagenetic modification of magnetic minerals, and only a few authors have once reported the formation of intermediate ferrimagnetic iron sulfide in the digenetic process of lake sediments[11]. A rock-magnetic investigation of the muddy sediments settled in the southeastern South Yellow Sea since about 13 ka BP is attempted here in order to ascertain the early diagenesis of the shelf sediments which is expected to have caused the profound modification of magnetic characteristics of the sediments, and to reveal the influence of changing post-glacial marine environmental conditions on the magnetic minerals diagenesis.

1 Geological setting and stratigraphy

The Yellow Sea is a semi-enclosed epicontinental sea between the Chinese mainland and the Korean Peninsula (fig. 1). Water depths in the Yellow Sea shelf range primarily between 20 and 80 m, except the Yellow Sea Trough whose maximum water depth is up to 140 m[12]. The Yellow Sea Warm Current (YSWC), a warm and saline water body, is a branch of the Tsushima Current, flows northwestward to enter the South Yellow Sea from the area southeast of the Cheju Island, and plays a key role in controlling the distribution of water masses and sedimentation in the Yellow Sea. There are 4 anti-clockwise cyclonic eddies along the sides of the YSWC (fig. 1). They are known as cold water masses or "cold eddies", occurring respectively in the northern East China Sea (southwest of Cheju Island), the central South Yellow Sea, the southeastern South Yellow Sea[13], and the western North Yellow Sea. The 4 cold eddies coincide with 4 muddy patches called "cyclonic eddy sediments"[14] or "muddy deposit of eddy"[15], and are generally considered to have been formed by the interaction among the YSWC, the Yellow Sea Coastal Current and Korean Peninsula Coastal Current.

Core YSDP103 (34°29.246′ N, 125°29.201′ E) was recovered in July 1995 in the muddy patch at the southeastern South Yellow Sea in a water depth of 53 m (fig. 1), as a fruit of research work conducted by Qingdao Institute of Marine Geology in cooperation with the Korean Institute of Geology, Mining & Mate

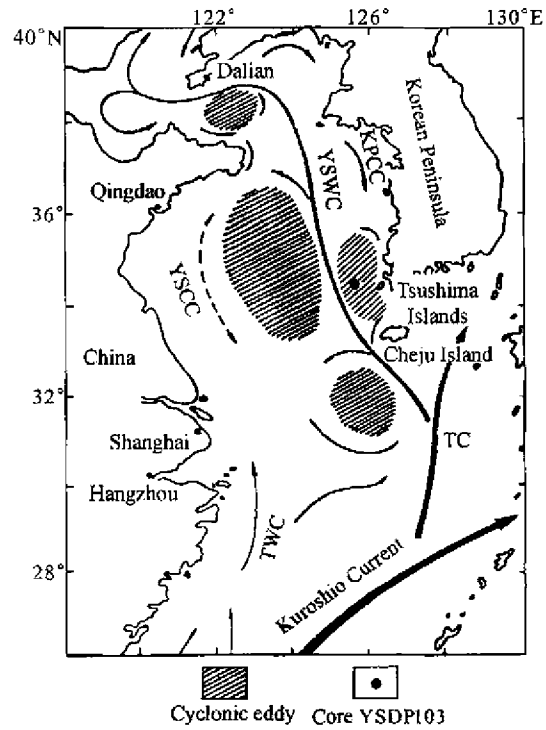

Fig. 1. Schematic map showing the location of core YSDP103 and the regional circulation pattern in the Yellow Sea and East China Sea (modified after ref. [14]). YSWC, Yellow Sea Warm Current; TC, Tsushima Current; YSCC, Yellow Sea Coastal Current; KPCC, Korean Peninsula Coastal Current; TWC, Taiwan Warm Current.

rial, Korea, yielding a 34.52-m-long core with the recovery of more than 90%. Previous studies[16, 17] have demonstrated that the total core can be stratigraphically divided into 3 sedimentary units as follows (in an ascending order): transgressive lag deposit (Unit C), tidal flat to beach deposit (Unit B), and shelf muddy deposit (Unit A) (fig. 2(a)), displaying a post-glacial transgressive sequence. Unit A, corresponding to the upper 29.79 m core, has been built up since about 13 ka BP based on ^{14}C datings and is composed of muddy sediments dominated by dark greenish grey (5G 4/1) to olive grey (5G Y4/1) clayey silts. The unit is generally homogeneous in color and lithology, though light grey silt and fine-grained sand laminae less than 0.5 mm thick, which were probably of storm origin, are intercalated in the muddy beds. Seismic profiles through the muddy patch in the southeastern South Yellow Sea also show that in Unit A there is a distinctive mid-reflector which divides the unit into two subunits, upper Unit A1 and lower Unit A2, and is

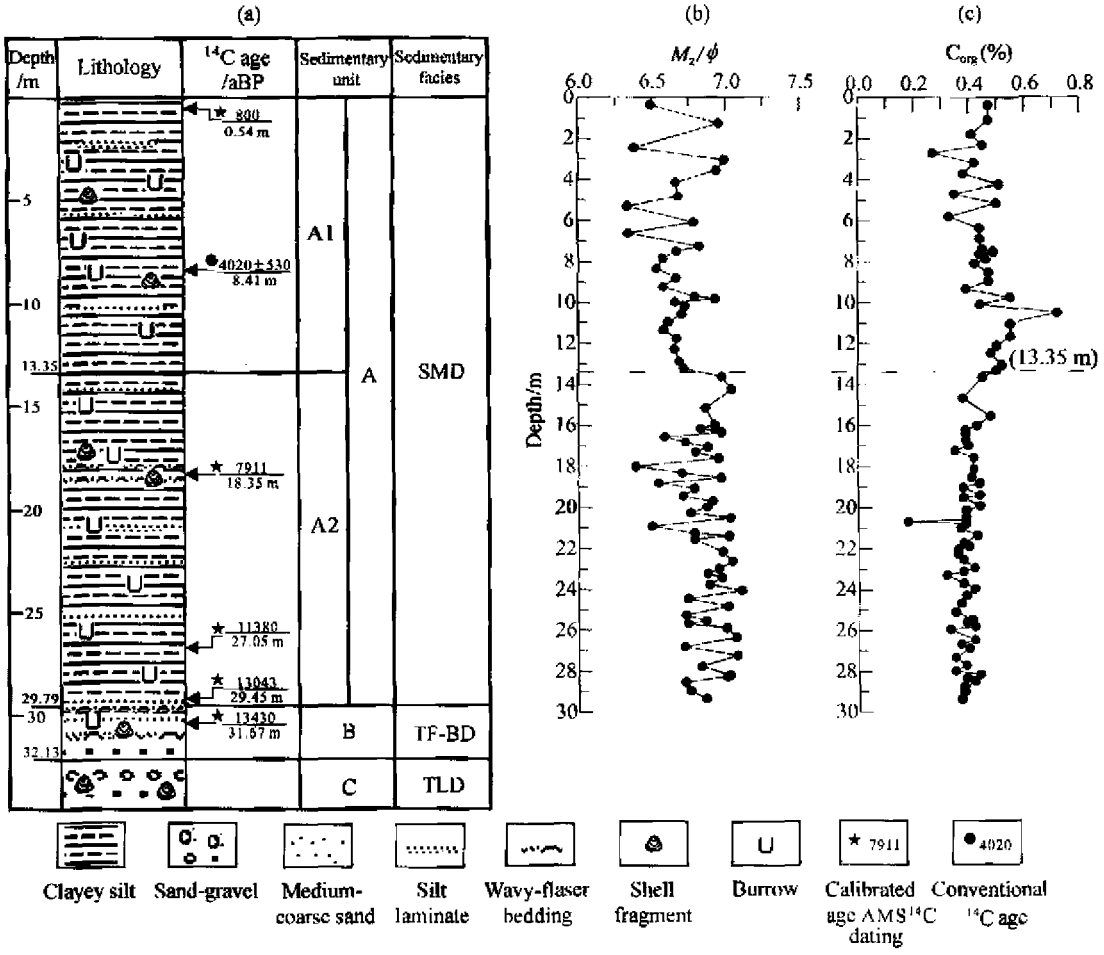

Fig. 2. (a) The sedimentary sequence and ^{14}C dating data of core YSDP103. (b) Downcore distributions of average grain size and (c) organic carbon content in the shelf muddy sediments of core YSDP103. AMS ^{14}C dates were measured with tests of foraminifera, and the calibrated ages were obtained by subtracting 400 years (an average ^{14}C age difference between the atmosphere and sea water[19]) from the measured AMS ^{14}C dates. ^{14}C dating by the conventional method was made using organic matter in the sediments. SMD, Shelf muddy deposit; TF-BD, tidal flat-beach deposit; TLD, transgressive lag deposit.

located at 13.35 m in core YSDP103 (fig. 2(a)). The core above 13.35 m is characterized by much higher water content than that below 13.35 m. Studies of the sedimentary features and downcore distributions of foraminifera in core YSDP103 and another drilling core to the south of core YSDP103, called core YSDP102 (retrieved in the same muddy patch)[17] suggest that the mid-reflector in Unit A corresponds to the Holocene maximum flooding surface at about 6 ^{14}C ka BP and signals the subsequent formation of the Yellow Sea Warm Current, and that Unit A1 was formed in the cold water mass occurring after the Yellow Sea Warm Current took shape.

2 Sampling and experimental methods

The uppermost 29.79 m of muddy sediments of core YSDP103 was used to carry out rock-magnetic investigation in this study. The core was split into halves, and sampled continuously along the axial line of one half with 8 cm^3 plastic cubes at intervals of 5—10 cm, yielding 315 samples in total from the upper 29.79 section. We avoided artificially disturbed core during sampling. Magnetic measurements of all samples were made at the laboratory of paleomagnetism of the Institute of Geology and Geophysics, CAS, Beijing. Measurements of magnetic susceptibility (χ), anhysteretic remanent magnetization (ARM), and iso-

thermal remanent magnetization (IRM) for the 315 samples were conducted successively.

Low-frequency volume-specific magnetic susceptibility was determined with a Bartington M.S. 2 susceptibility meter. ARMs were imparted in a GSD-1 Demagnetizer with an alternating peak field of 90 mT, superimposed by a direct bias field of 0.05 mT. IRMs were induced with a 2G660 pulse magnetizer in 1.6 T steady field in one direction, which are regarded here as Saturation IRMs (SIRMs). IRMs of 300 mT were then applied in the opposite direction, denoted as IRM_{-300}, and values of S_{300} (= $-IRM_{-300}/SIRM$) were calculated, which reflect the relative proportion of low- to high-coercivity minerals in samples. Measurements of all magnetic remanences were performed on a JR-5A Spinner Magnetometer. After above-mentioned magnetic parameters were measured the samples were oven-dried at 40℃ overnight and weighed to enable the calculation of mass-specific magnetic susceptibility (χ) and mass-specific values of ARM and SIRM.

The temperature dependence of magnetic susceptibility, namely χ(T) curve, was measured for representative sub-samples in heating-cooling cycles from room temperature to 700℃ using a KLY-3s kappa-bridge in an argon atmosphere. Partial sub-samples were used to carry out Lowrie's 3-axis IRM demagnetization experiment[7] by applying 2.7 T, 0.5 T and 0.05 T fields respectively along its 3 mutually perpendicular directions in a 2G660 pulse magnetizer, followed by thermal demagnetization in steps of 20—50℃ from 80℃ to 700℃ using a MMTD60 thermal demagnetizer, in order to measure the demagnetization behavior of various coercivity fractions in samples.

To a small number of samples from Unit A2, low-temperature remanence measurements were given using a Quantum Design MPMS 2 manetic-properties measurement system at the Institute for Rock Magnetism, University of Minnesota, USA. First, a sample was cooled in zero applied field from room temperature to 20 K, and then exposed to a 2.5 T field to impart SIRM at 20 K, and finally changes in SIRM were automatically recorded as the sample was heated back to room temperature in zero field.

After all magnetic measurements as noted above, 83 of the total 315 samples were selected at intervals of 0.2—0.7 m to analyse their organic carbon content using a LecoCS-34 Carbon/sulphur Determinator at Wuxi Institute of Experimental Geology, Research Institute of Petroleum Exploration and Production, SINOPEC, with data precision better than 0.01%. Additionally, 75 of all the magnetic samples were taken at 0.2—1.2 m intervals to determine grain sizes in the Experiment-Testing Center of Marine Geology, Qingdao Institute of Marine Geology with a laser particle size analyzer, Mastersizer-2000, which was made in the Malvern Compony of England.

3 Results

3.1 Downcore distributions of gain size and organic carbon content

The average grain sizes of the uppermost 29.79 m range between 6.3ϕ and 7.2ϕ (fig. 2(b)), indicating a roughly constant grain-size distribution downcore, which is consistent with our visual observation. Except at one level, organic carbon content is relatively invariable in Unit A2, averaging 0.39%, whereas in Unit A1 it increases notably both in absolute value and extent and is 0.46% on the average (fig. 2(c)).

3.2 Downcore changes of magnetic parameters

Figure 3 shows variations of χ, ARM, SIRM and S_{300} with depth in Unit A of core YSDP103. In Unit A1 above 13.35 m, the 4 parameters display a large and precipitous drop in values from 2.35 downward to 4.60 m, whereupon they continue to decrease slightly or remain roughly constant downcore up to 13.35 m. Compared with the values in the uppermost 2.35 m, χ, SIRM and ARM in the interval from 4.60 to 13.35 m decrease by 40%, 60% and 85% on the average, respectively. Values of S_{300} in the upper 2.35 m range between 0.87 and 0.93, suggesting that the sediment is dominated in magnetic mineralogy by low-coercivity minerals with a small content of high-coercivity minerals scattered; they decline markedly downcore from 2.35 m, attaining around 0.75 at 4.60 m, which indi-

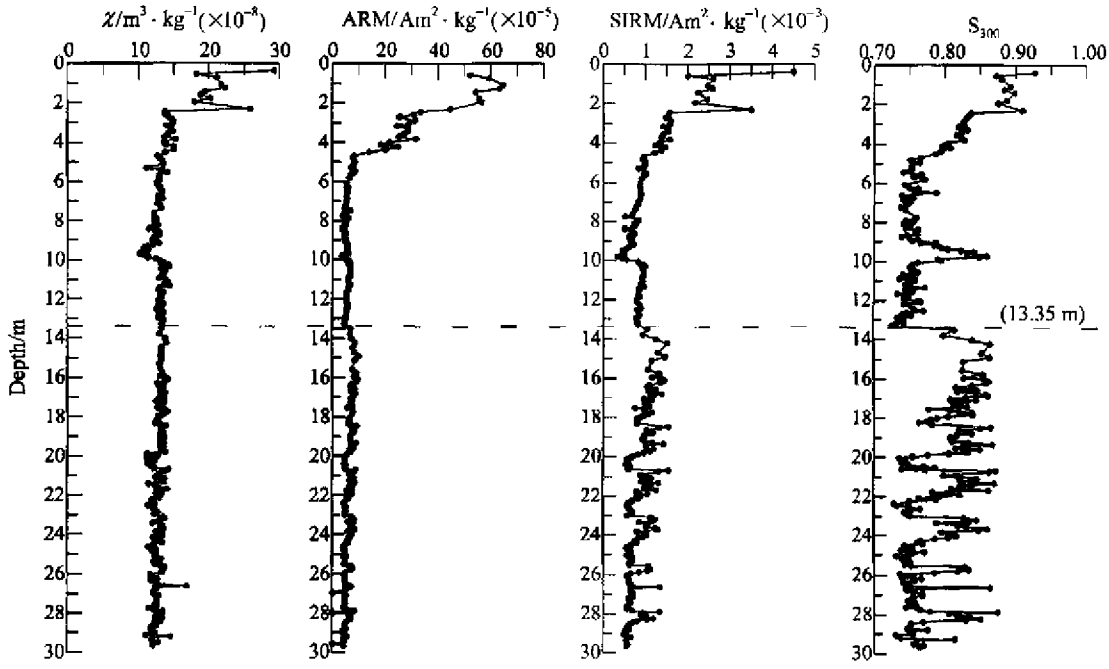

Fig. 3. variations of χ, ARM, SIRM and S_{300} in the uppermost 29.73 m of core YSDP103.

cates that low-coercivity minerals fall dramatically below 2.35 m and that high-coercivity minerals are predominant between 4.60 and 13.35 m (except in the interval from 9.20 to 10.00 m).

Due to relatively uniform lithology throughout the muddy core, the changing patterns of the 4 parameters above 13.35 m can be regarded as the magnetic properties diagnostic of diagenesis in sedimentary sequences[1,7–9], reflecting a diagenetic process resulting in the remarkable drop in magnetic mineral content and in preferential dissolution of fine-grained low-coercivity minerals downcore from 2.35 m. The increasing proportional loss of χ, SIRM and ARM can be ascribed to their enhancing sensitive degree to the loss of low-coercivity magnetic minerals in the same order. Convincing evidence in support of diagenesis in the core is a small amount of authigenic pyrite commonly seen in the middle to lower core. Many studies have shown that magnetic mineral diagenesis begins with iron oxide reduction, leading to an initial dissolution of the finest-grained iron oxides (largely low-coercivity gains such as magnetite) followed by the destruction of the remaining coarse grains[11]. In this diagenetic stage, ferric (Fe^{3+}) ions dissociated from iron oxides are reduced into the divalent state. The later stage of magnetic mineral diagenesis is sulphate reduction, in which dissolved ferrous (Fe^{2+}) ions may react with H_2S, whose most important source is the reduction of interstitial dissolved sulphate by bacteria that use organic matter as a reducing agent, to form a succession of iron sulphide phases. In this process, formations of iron sulphides from aqueous solution are in the following order: mackinawite (with a composition similar to $FeS_{0.9}$), pyrrhotite (hexagonal $Fe_{11}S_{12}$ to Fe_9S_{10} and monoclinic Fe_7S_8), greigite (Fe_3S_4), and finally pyrite[21]. Mackinawite, pyrrhotite and greigite are thermodynamically metastable relative to pyrite, and may further react with element sulphur to form pyrite, the most stable iron sulphide phase under reducing conditions. Among the iron sulphides, only monoclinic pyrrhotite and greigite are ferrimagnetic and capable of carrying a magnetic remanence.

In Unit A2 between 13.35 and 29.73 m, the 4 magnetic parameters show a generally progressive decline in values with depth though the fall in values of χ is least obvious. With the exception of χ, all the parameters exhibit distinct changes from below to

above 13.35 m. It is worth notice that the changing trends of the 4 parameters are superimposed by 6 zones with higher values. This is most striking in the S_{300} profile, with lower-values (0.72 to 0.77) and higher-values (0.80 to 0.87) zones alternating and showing a progressive decline downwards in the overall trend. Values of S_{300} drop sharply from 13.35 m upwards. Positive correlations are observed among the 4 parameters, consistent with the preferential dissolution of low-coercivity magnetic minerals in the diagenetic process.

3.3 Magnetic mineralogy

Magnetic components in different intervals of the shelf muddy deposit in core YSDP103 are analysed below according to Lowrie's 3-axis IRM demagnetization experiment, χ(T) curves and low-temperature remanence measurements of the samples.

0 to 2.35 m: The Lowrie's 3-axis magnetization experiment on samples from this interval indicates that unblocking of the low-coercivity fraction (less than 0.0.5 T) occurs around 580℃ (fig. 4(a)), pinpointing magnetite as its carrier of remanent magnetization. The medium-coercivity fraction (0.05 to 0.5 T) shows two evident unblockings at about 580℃ and 680℃, characteristic of magnetite and hematite, respectively; it also shows rapid decay between 120 and 320℃, probably reflecting the presence of maghemite[22]. The high-coercivity fraction (0.5 to 2.7 T) exhibits its unblocking at about 680℃, indicative of hematite. The χ(T) curve (fig. 5(a)) basically keeps constant or shows a very slight increase from room temperature to about 300℃, and then rise slowly until around 440℃ presumably due to the thermally induced conversion from iron-bearing silicate or clay minerals to new magnetite[23]. The susceptibility decreases slowly from 440 to 550℃, likely resulting from the conversion of maghemite into hematite, and then drops abruptly

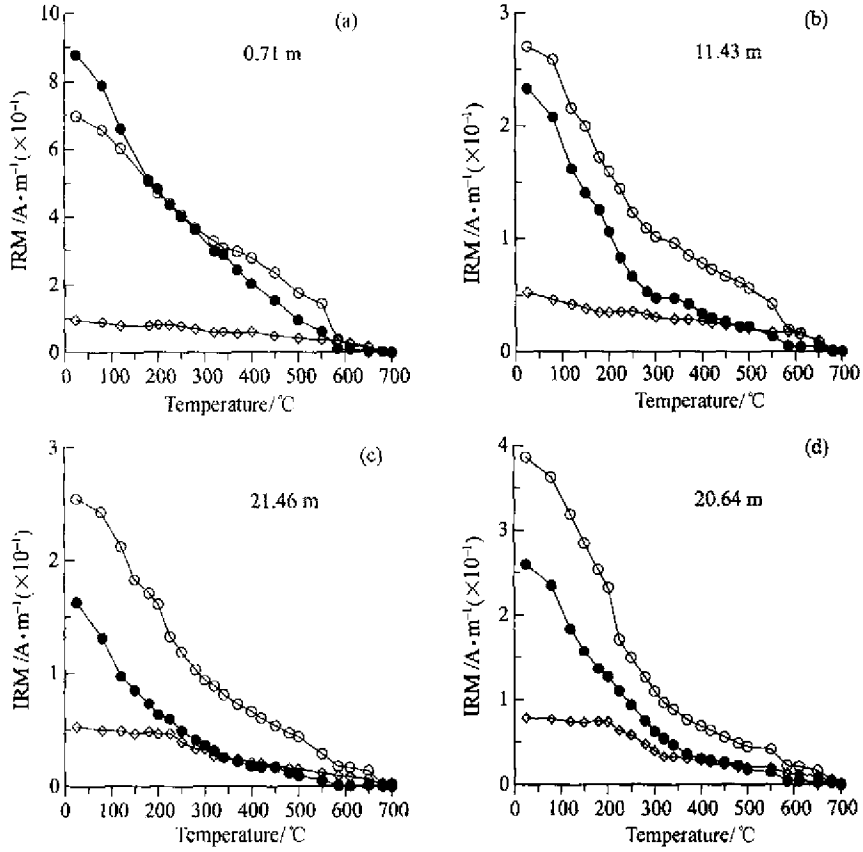

Fig. 4. Thermal demagnetizations of a 3-axis IRM in samples from different intervals in core YSDP103. (a) Samples in 0 to 2.35 m. (b) Samples in 2.35 to 13.35 m. (c) and (d) Samples in 13.35 to 29.73 m. ◇, 2.7—0.5 T; ○, 0.5—0.05 T; ●, <0.05 T.

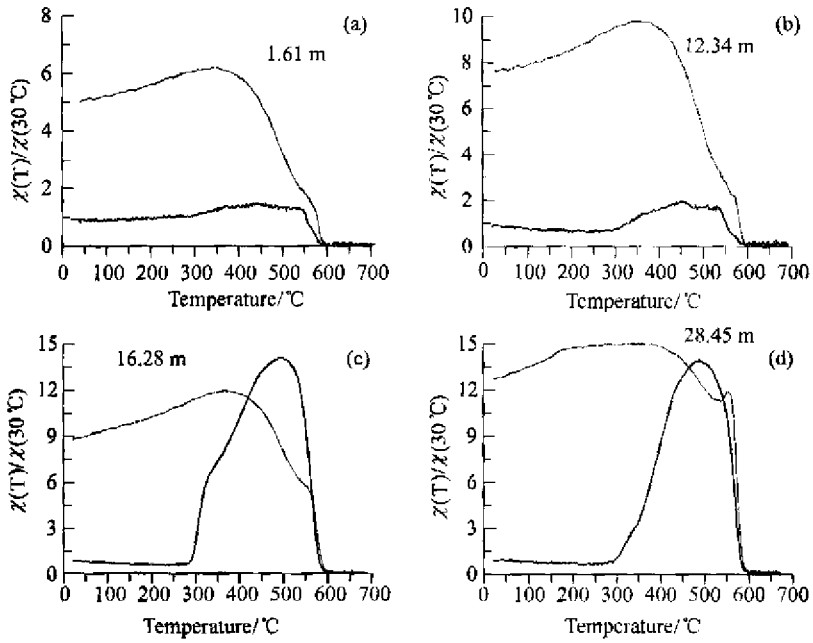

Fig. 5. Typical high-temperature dependence of magnetic susceptibility for samples in different intervals of core YSDP103. (a) Samples in 0 to 2.35 m. (b) Samples in 2.35 to 13.35 m. (c) and (d) Samples in 13.35 to 29.73 m. Thick and thin lines stand for heating and cooling processes, respectively. The *Y*-axis values of each sample are the χ (T) normalized by χ (30℃).

above ~550℃ to nearly zero at ~580℃, consistent with a magnetite Curie temperature. On cooling a major increase in χ occurs rapidly from 580 to 350℃; below 350℃ χ decreases slowly until room temperature is reached. When all these finished, the χ value has been about a five-fold increase compared to the pre-heating value, suggesting the production of a large magnetite phase during the heating-cooling cycle. In summary, the above experimental results confirm that in this interval (0—2.35 m) which is basically free from diagenesis the magnetic mineralogy is dominated by magnetite besides maghemite and hematite.

2.35 to 13.35 m: The 3-axis magnetization experiment on samples in this interval yields similar results to those of the above 2.35 m samples, but the low-coercivity fraction covers a much smaller portion of the total IRM (consistent with great diagenetic dissolution of magnetic minerals in the core), which is obviously different from the samples above 2.35 m. The χ(T) curve (fig. 5(b)) shows that χ decreases slowly from room temperature to around 300℃, a contribution of the presence of paramagnetic minerals, presumably due to formation of paramagnetic pyrite in the diagenetic modification of magnetic minerals. This is followed by a notable increase in χ from 300 to 460℃, which can be caused partially by the thermally induced conversion of iron-bearing silicate or clay minerals into magnetite and partially by the conversion of newly formed paramagnetic pyrite during diagenesis into magnetite within this temperature range[24]. A gradual, slight decrease in χ is observed from 460℃ up to 550℃, as is expected for the high temperature behavior of maghemite, and the decrease of χ accelerates above 550℃ until zero is reached at ~580℃, corresponding to the Curie temperature of magnetite. During cooling, χ behaves in a similar way to that in the interval above 2.35 m, but the χ value at room temperature comes to be seven times larger than the pre-heating one, greater than in the uppermost 2.35 m section, probably owing to pyrite formed in the diagenetic process. In brief, the above experimental results suggest that magnetite, maghemite and hematite are the main magnetic minerals in this interval (2.35 to 13.35 m), with a much lower proportion of magnetite than in the uppermost 2.35 m.

13.35 to 29.73 m: Samples both from higher-S_{300} and lower-S_{300} zones give very similar 3-axis magnetization experiment results and χ(T) curves. In the 3-axis magnetization experiment (fig. 4(c) and (d)), the most distinct difference from that of the overlying section is that both the high- and the medium-coercivity fraction show a considerable decrease from 220 ℃ to 320 ℃ though the loss in the high-coercivity fraction is more pronounced. And the low-coercivity fraction shows a significant reduction between 100℃ and 400℃. Since greigite is characterized by loss of most of its magnetization from 200℃ to 350℃[20,25,26], we can attribute the rapid decay of magnetization in the high- and midium-coercivity fractions within the temperature window of 200—320℃ to the presence of greigite. This kind of thermomagnetic behavior may be due to the fact that greigite is subject to a maximum of thermal decomposition at around 200℃ and gets to its Curie temperature at about 320℃, in contrast to the thermomagnetic behavior of pyrrhotite which shows rapid unblocking within a much narrower temperature range of 320—350 ℃ [20,26]. Moreover, the behavior of high-coercivity fraction rules out the possibility that the loss in magnetization around 200—320℃ is due to the presence of maghematite or titanomagnetite. And the high temperature behavior of low-coercivity fraction can be attributed to the likelihood that the thermal demagnetizaiton of greigite is obscured by the thermal instability of maghematite and/or titanomagneitte. The χ(T) curve of heating shows a marked rise from ~300℃ to abou 500℃ and then an abrupt decrease from 500℃ to 580℃ at which the Curie temperature arrives (fig. 5(c) and (d)). The increase in χ at ~300℃ is characteristic of greigite, probably signaling the onset of thermal alteration of greigite into magnetite or maghemite[27]. The low-temperature measurement bears evidence of a Verwey transition at about 120 K (fig. 5), diagnostic of magnetite[28], but does not show any phase transition between 30 K and 40 K, an indicator of pyrrhotite[29]. In short, the above results can lead to the conclusion that the magnetic minerals in this interval (13.35 to 29.73 m) contain greigite, besides magnetite, maghemite and hematite as is the case in the uppermost 13.35 m section.

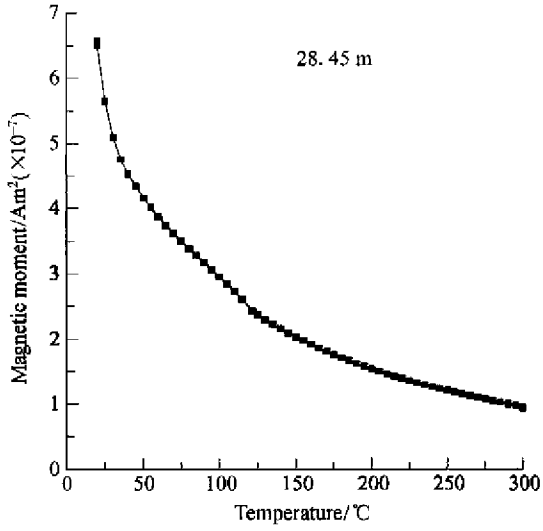

Fig. 6. Low-temperature measurement of the sample from the interval of 13.35—29.79 m in core YSDP103. The magnetite Verwey transition at about 120 K can be seen, but no magnetic phase transition between 30 and 40 K indicative of pyrrhotite is observed.

4 Discussion

Previous studies[21] have shown that during the early diagenesis in sediments three principal factors control pyrite formation and preservation of ferrimagnetic iron sulphides: the availability of dissolved sulphate, iron in detrital minerals which reacts with H_2S to form iron sulphide minerals, and decomposable organic matter. Sagnotti et al. (2001)[30] suggested that the first two factors should not be the diagenetic constrains in normal marine environments and that the amount of available organic matter acts as the controlling factor on the diagenetic products of magnetic minerals in marine sediments. Roberts et al. (1996)[5], in his study of greigite in several horizons of paleo-lake beds, put forward that residence time of lake water was related to varying degrees to whether the lake basin was open or closed, and the longer the residence time, the richer the accumulation of sulphate, which could greatly affect the formation of diagenetic products of magnetic minerals. Of the muddy sediments from 0 to 29.79 m in core YSDP103, the lower part (Unit A2) was formed during the fast post-glacial transgression until the middle Holocene (at about 6

^{14}C ka BP) when the sea level rose to its maximum, whereas the upper part (Unit A1) was deposited in a cold-eddy environment associated with the formation of the Yellow Sea Warm Current after the middle-Holocene maximum sea level. Therefore the sediments of Unit A1 were settled in a more reductive environment than those of Unit A2 accumulated[14], as is evidenced by a difference in organic carbon content between the two sections. Furthermore, marine water where Unit A2 was formed should be more mobile and thus had shorter residence time than the cold-eddy water from which Unit A1 was laid down. Based on the above analyses, we think that the distinction between Unit A1 and Unit A2 in the factors controlling the magnetic mineral diagenensis is that the former has more organic matter and sulphate involved in, leading to complete conversion into pyrite, of the intermediate product (greigite), while the latter only obtains partial conversion due to the less amount of organic matter and sulphate.

Downcore variations of the multiple magnetic parameters in the muddy section (Units A1 and A2) of core YSDP103 suggest a gradually downward decreasing of both magnetic concentration and proportion of low- to high-coercivity minerals, or in other words, suggest a progressively strengthening of magnetic mineral diagenesis with depth. The abrupt changes in magnetic content and components at 13.3 m of the core are thought to have been caused by alteration of sedimentary environment and also, to some extent, provenance after the Yellow Sea Warm Current came into being[17]. In detail, the original composition, concentration and grain sizes of the magnetic minerals differ between Unit A1 and Unit A2, that is to say, the diagenesis of each section took place on a different material base and in different environmental conditions.

The organic carbon content in Unit A2 of core YSDP103 is relatively invariable, and shows no correlation with changes of magnetic parameters (see figs. 2 and 3), suggesting that the fluctuations of magnetic parameters may not result from the changes of diagenetic environment. Accordingly, we speculate that the major reason for the observed alternations of zones of high and low magnetic parameters in Unit A2 is that during the deposition of the section detrital magnetic mineral supplies to the study area alternated between relatively rich and/or coarse-grained magnetic minerals and relatively poor and/or fine-grained ones, which correspond to the higher and lower magnetic parameters zones, respectively. Because the muddy sediments in the southeastern South Yellow Sea have complex sources[17], further work needs to be done to reveal what factors, climatic or non-climatic, have governed the variations of content and grain sizes of magnetic minerals discharged into the study area during the formation of Unit A2.

As to the unusual increase of S_{300} from 9.2 to 10.0 m in Unit A1, considering the corresponding χ and SIRM values are the lowest in the same section, we think that it can be reasonably interpreted by the strongest diagenesis occurring in the bed, which resulted in dissolution of large proportion of high-coercivity magnetic minerals as well as low-coercivity minerals (presumably fine-grained) and thus the rise of S_{300} values.

5 Conclusions

(1) The shelf muddy sediments formed during the last ~13 ka in the southeastern South Yellow Sea, as was recovered in core YSDP103, are characterized by a magnetic mineralogy dominated by magnetite, maghemite and hematite. Except for the uppermost 2.35 m, the muddy sediments were subject to reductive diagenesis, including iron oxides reduction (dissolution of magnetic grains) and sulphate reduction (formation of pyrite), consequently leading to a significant decrease of magnetic components as is suggested by as much as 40% to 85% drop in values of χ, ARM and SIRM and also a simultaneously considerable decrease in the proportion of low-coercivity magnetic minerals.

(2) The muddy sediments corresponding to Unit A2 in core YSDP103, formed from the initial post-glacial transgression (at about 13 ka BP) to the Holocene sea-level maximum (at about 6 ^{14}C ka BP), retain ferrimagnetic iron sulphide (greigite), but the muddy sediments corresponding to Unit A1 in the core,

deposited in a cold-eddy environment associated with the formation of the Yellow Sea Warm Current after about 6 ka BP, are devoid of ferrimagnetic iron sulphide. This indicates the controlling of environmental conditions on the diagenetic changes of magnetic minerals. Abrupt variations of magnetic parameters occur across the Unit A1/A2 boundary, which is interpreted to reflect a joint influence of environmental conditions and original magnetic compositions on the diagenesis.

(3) Alternating zones of high and low magnetic parameters are observed in Unit A2 of core YSDP103, which is presumably due to periodic changes of the concentration and/or grain size of magnetic minerals carried into the study area.

Acknowledgements This work was supported by the National Natural Science Foundation of China (Grant Nos. 49976012 and 49736210). We are grateful to Dr. M. Jackson with the Institute for Rock Magnetism, University of Minnesota, USA for his help with the low-temperature remanence measurement. We also wish to thank Dr. Pan Yongxin with the Institute of Geology and Geophysics, CGS for his careful and valuable comments.

References

1. Karlin, R., Levi, S., Diagenesis of magnetic minerals in recent hemipelagic sediments, Nature, 1983, 303: 327—330.
2. Canfield, D. E., Berner, R. A., Dissolution and pyritization of magnetite in anoxic marine sediments, Geochim. Cosmochim. Acta, 1987, 51: 645—660.
3. Liu, J., Reductive diagenesis of magnetic minerals: A review, Marine Geology & Quaternary Geology (in Chinese with English abstract), 2000, 20(4): 103—107.
4. Sagnotti, L., Winkler A. Rock magnetism and palaeomagnetism of greigite-bearing mudstones in the Italian peninsula, Earth and Planetary Science Letters, 1999, 165: 67—80.
5. Roberts, A. P., Reynolds, R. L., Verosub, K. L. et al., Environmental magnetic implications of greigite (Fe3S4) formation in a 3 m.y. lake sediment record from Butte Valley, northern California, Geophys. Res. Lett., 1996, 23: 2859—2862.
6. Ariztegui, D., Dobson, J., Magnetic investigations of framboidal greigite formation: a records of anthropogenic environmental changes in eutrophic Lake St Moritz, Switzerland, The Holocene, 1996, 6: 235—241.
7. Karlin, R., Magnetite Diagenesis in marine sediments from the Oregon continental margin, Journal of Geophysical Research, 1990, 95(B4): 4405—4419.
8. Leslie, B. W., Lund, S., Hammond, D. E., Rock magnetic evidence for the dissolution and authigenic growth of magnetic minerals within anoxic marine sediments of the California continental Borderland, Journal of Geophysical Research, 1990, 95(B4): 4437—4452.
9. Karlin, R., Lyle, M., Heath, G. R., Authigenic magnetite formation in suboxic marine sediments, Nature, 1987, 326: 490—493.
10. Stockhausen, H., Thouveny, N., Rock-magnetic properties of Eemian maar lake sediments from Massif Central, France: a climatic signature? Earth and Planetary Science Letters, 1999, 173: 299—313.
11. Hu, S., Appel, E., Hoffmann, V. et al., Identification of greigite in lake sediments and its magnetic significance, Science in China, Ser. D, 2002, 45(1): 81—87.
12. Qin, Y., Zhao, Y., Chen L. et al., Geology of The Yellow Sea (in Chinese with English abstract), Beijing: Ocean Press, 1989.
13. Lan, S., Gu, C., Fu, B., A study of cold water body near the southern Yellow Sea Warm Current water, Studia Marina Sinica (in Chinese with English abstract), 1986, (27): 55—64.
14. Shen, S.X., Chen, L.R., Gao, L. et al., Discovery of Holocene cyclonic eddy sediment and pathway sediment in the southern Yellow Sea, Oceanologia et Limnologia Sinica (in Chinese with English abstract), 1993, 24(6): 563—570.
15. Li, S. Q., Liu, J., Wang, S.J. et al., Sedimentary characters in the eastern South Yellow Sea during the post-glacial transgression (in Chinese with English abstract), Marine Geology & Quaternary Geology, 1997, 17(4): 1—12.
16. Li, S. Q., Liu, J., Wang, S. J. et al., Sedimentary sequence and environmental evolution in the eastern south Yelow Sea during the last deglaciaiton and the Holocene, Chinese Science Bulletin, 1998, 43(9): 757—761.
17. Liu, J., Li, S. Q., Wang, S. J., Sea level changes of the Yellow Sea and formation of the Yellow Sea Warm Current since the last Deglaciaton, Marine Gelogy and Quaternary Geology (in Chinese with English abstract), 1999, 19(1): 13—24.
18. Jin, J. H., Chough, S. K., Partitioning of transgressive deposits in the southeastern Yellow Sea: a sequence stratigraphic interpretation, Marine Geology, 1998, 149: 79—92.
19. Bard, E., Correlation of accelerator mass spectrometry ^{14}C ages measured in planktonic foraminifera: Paleoceanographic implications, Pleoceanography, 1988, 3: 635—645.
20. Lowrie, W., Identification of ferromagnetic minerals in a rock by coercivity and unblocking temperature properties, Geophys, Res. Lett., 1990, 17: 159—162.
21. Berner, R. A., Sedimentary pyrite formation: an update, Geochim. Cosmochim. Acta, 1984, 48: 605—615.

22. Zhu, R. X., Shi, C. D., Suchy, V. et al., Magnetic properties and paleoclimatic implications of loess-paleosol sequences of Czech Republic, Science in China, Ser. D, 2001, 44(5): 385—394.
23. Zhu, R., Kazansky, A., Matasova, G. et al., Rock-magnetic investigation of Siberia loess and its implication, Chinese Science Bulletin, 2000, 45(23): 2192—2197.
24. Roberts, A. P., Pillans, B. J., Rock magnetism of Lower/Middle Pleistocene marine sediments, Wangnui Basin, New Zealand, Geophys. Res. Lett., 1993, 20: 839—842.
25. Snowball, I. F., Magnetic hysteresis properties of greigite (Fe3S4) and a new occurrence in Holocene sediments from Swedish Lappland, Phys. Earth Planet. Inter., 1991, 68: 32—40.
26. Torii, M., Fukuma, K., Hong, C. -S. et al., Magnetic discrimination of pyrrhotite- and greigite-bearing sediment samples, Geophys. Res. Lett., 1996, 23: 1813—1816.
27. Geiss, C. E., Banerjee, S. K., A multi-parameter rock magnetic record of the last glacial-interglacial paleoclimate from south-central Illinois, USA, Earth and Planetary Science Letters, 1997, 152: 203—216.
28. Ozdemir, O., Dunlop, D. J., Moskowitz, B. M., The effect of Oxidation on the Verwey transition in magnetite, Geophys, Res. Lett., 1995, 134: 227—236.
29. Rochette, P., Fillion, F., Mattei, J. L. et al., Magnetic transition at 30-40 kelvin in pyrrhotite: insight into a widespread occurrence of the mineral in rocks, Earth and Planetary Science Letters, 1990, 98: 319—328.
30. Sagnotti, L., Macri, P., Camerlenghi, A. et al., Environmental magnetism of Antarctic late Pleistocene sediments and interhemispheric correlation of climatic events, Earth and Planetary Science Letters, 2001, 192: 65—80.